Acta Mech
DOI 10.1007/s00707-013-1020-1

Sayed-Mahdi Hashemi-Dehkordi · Pier Paolo Valentini

Comparison between Bezier and Hermite cubic interpolants in elastic spline formulations

Received: 2 August 2013 / Revised: 1 October 2013
© Springer-Verlag Wien 2013

Abstract In this paper, a comparison between two different formulations of elastic splines is made. The two methods under investigation are based on the Bézier and Hermite interpolants. The strategies have been implemented and compared using two simulation cases involving medium and large deflections of a slender element. The investigation has been carried out considering the same number of degrees of freedom, and the two approaches have been compared in terms of complexity, accuracy and robustness. Both methods have also been compared with nonlinear finite element models.

1 Introduction

The use of spline entities for addressing flexible beam simulations has been introduced by Quin and Terzopoulos in 1996 [1] and then optimized and specialized by several authors in different application fields. The main idea is using a mathematical representation of the beam neutral axis using an oriented curve that passes through the center of every cross section described by a computer-aided design formulation, able to combine physical-based constraining equations with spline geometry representation. Thanks to this feature, a complex and large displacement field of a beam-shaped element can be expressed in terms of closed-form polynomials using the well-known spline description [2], deducing geometrically exact expressions of kinetic and elastic energies. This modeling strategy has been the basis for the modern isogeometric analysis [3], involving the use of the same representation for modeling and simulating form 1D to 3D structures.

Limiting the brief overview of the relevant contributions of these simulation strategies in the field of beam modeling, in 2006, Cottrell et al. [4] presented an application of isogeometric analysis for structural vibrations. In 2008, Theetten et al. [5] proposed an optimized formulation suitable for plastic deformations. In 2010, Nagy et al. [6] proposed a sizing and shape optimization algorithm based on an isogeometric beam. In the same year, Benson et al. [7] discussed the implementation of a generalized formulation suitable for structural investigations based on arbitrary basis functions. In 2011, Valentini and Pennestrì [8] specialized and tested the formulation of elastic splines for multibody dynamics simulations. Other applications of elastic splines have been proposed in the field of compliant mechanisms [9] and biomechanics [10] and testify an increasing importance of the methodologies. In 2012, Bouclier et al. [11] investigated the use of higher-order NURBS to address static straight and curved Timoshenko beam with several approaches. More recently, Raknes et al. [12] studied the statics and dynamics behavior of cables using a similar approach, and Weeger et al. [13] implemented and Euler–Bernoulli beam model for vibration analysis.

All these contributions confirm an increasing interest of the scientific community in such numerical methods especially in the fields of engineering and technical design.

S.-M. Hashemi-Dehkordi (✉) · P. P. Valentini
Department of Enterprise Engineering, University of Rome "Tor Vergata", Via del Politecnico, 1, 00133 Rome, Italy
E-mail: mhpath3@gmail.com; Hashemi.Dehkordi@ing.uniroma2.it; s.mahdi.hashemi.d@gmail.com

Published online: 27 November 2013

Most of the above-mentioned applications are based on the representation of one-dimensional objects using the same spline formulation, which is very common in computer-aided design [2]. A spline is a piecewise polynomial description of a curve in parametric form. Each piece is connected to the adjacent ones by respecting a parametric and geometric continuity. The shape is controlled by geometrical entities (points or slopes) interpolated with specific blending functions.

In general, the blending functions depend on the degree of the polynomials (two or three in general cases), on the type of control pieces of information and regularity parameters [2]. In order to increase the capabilities in describing complex shapes, the blending functions may be weighed using coefficients producing the weighted rational averages.

The control pieces of information can be considered the degrees of freedom of the spline. In many cases, these variables do not have a direct physical meaning (as it happens for the nodes in the finite element approach), but are mere mathematical entities that can also be external from the modeled shape.

In comparison with finite element approaches, elastic splines allow the use of the same representation for drawing and simulating without requiring the meshing (discretization) of flexible parts. Since the shape and the displacement of a spline can be described in terms of control points, elastic splines allow accurate modeling requiring a reduced number of variables (degrees of freedom) and using an absolute coordinate description as in the ANCF formulations [14–17]. Although the ANCF approach may make use of both nodal coordinates and slopes [15], the concept is from that of the dynamic spline since there is no direct relationship between geometrical entities and analysis entities, which is guaranteed by specific shape continuity. Moreover, thanks to the continuity of the piecewise description of the shape, elastic splines allow better continuity of both displacement and stress fields, which it is often not possible with standard finite element formulations.

Although the basic idea behind the elastic spline approach is almost the same, the practical implementation can be different. The most relevant differences are in the choice of the degree of polynomial functions and in the type of the control pieces of information. In order to have a good trade-off between simplicity and accuracy, the choice of the degree of the polynomial function is limited between two and three. On the other side, several strategies in the interpolation of the control pieces of information can be used. For examples, Theetten et al. [5] proposed to use the Catmull–Rom blending functions, Valentini and Pennestrì [8] the cubic Bézier form or a hybrid point/slopes formulation [9]. These approaches are very general and may be suitable for addressing many practical problems, allowing the possibility of including a large number of control points.

The motivations of this paper arise from the need of having a direct comparison between two of the most important formulations (Bézier spline and Hérmite spline interpolation techniques) in order to have an assessment of the accuracy, computational complexity and capability in simulating nonlinear and highly nonlinear scenarios in planar statics. The two methodologies are compared in both a simple and a complex scenario in order to find out the benefits and drawbacks of each one. To the authors best knowledge, this type of comparison has been never addressed, so it can be considered a novelty.

Concerning the organization of the paper, in the first part, a brief recall of both interpolation methods is presented. In the second part, the details of elastic spline implementation are discussed. In the third part, a comparison concerning two different simulation scenarios is addressed focusing on the differences between the two approaches.

2 Spline formulations

Two different formulations have been compared in this study: the Bézier spline and the Hermite spline. They both rely on the use of computer-aided geometrical description of curves. Although the bases of these definitions are well known, some recalls have been included in order to make this paper self-contained.

2.1 Bézier spline (B-spline)

A piecewise parametric curve $p(u)$ described with Bézier's formulation can be deduced considering a set of $m - n + 1$ control points, $\{P_0, P_1, \ldots, P_{m-n+1}\}$ using the following formula [2]:

$$p(u) = \sum_{j=0}^{m-n} b_{j,n}(u) P_j \qquad t_n \leq u \leq t_{m-n+1}, \tag{1}$$

where

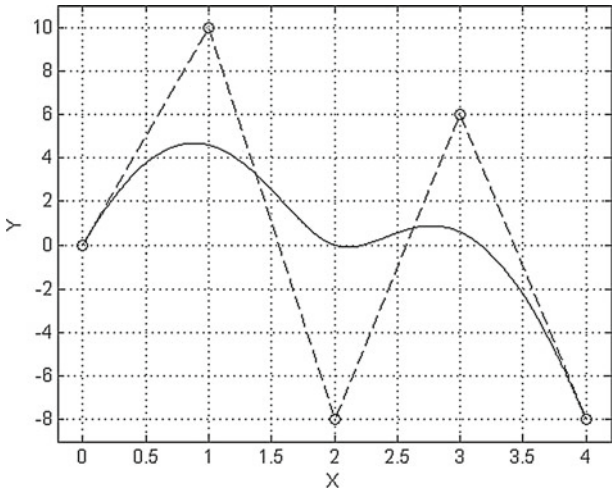

Fig. 1 An example of B-spline with 5 control points

m is the number of knots, equal to the number of the segments of the curve plus one;
n is the polynomial degree of the blending functions. In this investigation, we use cubic interpolants, thus $n = 3$.
$b_{j,n}(u)$ are the blending functions (polynomial functions of the variable u) fitting the control points;
t_n are the knots (the values of the variable u when passing from one segment of the piecewise polynomial to another) that can be chosen regularly spaced. In order to guarantee that the curve passes through the first and last control point (quite a common and useful situation), the first and last knots are repeated as many times as the degree of the polynomial (3 in our case).

The blending functions $b_{j,n}$ can be computed using the following recursive formula which involves the knot sequence:

$$b_{j,n}(u) = \frac{u - t_j}{t_{j+n} - t_j} b_{j,n-1}(u) + \frac{t_{j+n+1} - u}{t_{j+n+1} - t_{j+1}} b_{j+1,n-1}(u) \tag{2}$$

under the conditions:

$$\begin{aligned} b_{j,0}(u) &= 1 \quad t_j \le u < t_{j+1}, \\ b_{j,0}(u) &= 0 \quad \text{elsewhere.} \end{aligned}$$

The control points can be considered as the degrees of freedom of the spline. Each control point possesses two degrees of freedom (x and y translations) in two-dimensional simulations and four degrees of freedom (x, y and z translations and torsion θ) in three-dimensional simulations. According to the blending functions definition in Eq. (2) and the repetition (multiplicity) of the knots, except for the first and the last control point, the curve does not pass through them, but their position in space influences the shape of the spline. Since most of them do not belong to the curve, these control variables do not have a direct physical meaning, but are mere mathematical entities.

Figure 1 shows a B-spline with 5 control points, with the following coordinates: $P_x = \{0.0 \quad 1.0 \quad 2.0 \quad 3.0 \quad 4.0\}^{\mathrm{T}}$ and $P_y = \left\{0.0 \quad 10.0 \quad -8.0 \quad 6.0 \quad -8.0\right\}^{\mathrm{T}}$ (Fig. 2).

2.2 Hermite spline (H-spline)

The Hermite spline is defined trough a set $\left\{P_0, P_0', P_1, P_1', , \ldots, P_n, P_n'\right\}$ of interpolation points P_i and their tangent vectors (slopes) P_i'. In this case, the points physically belong to the curve. Each interpolation point has four degrees of freedom (x and y translations x' and y' slopes) in two-dimensional simulations and seven degrees of freedom (x, y and z translations, x′, y' and z' slopes and torsion θ) in spatial simulation.

The Hermite spline is defined for a span consisting of two control points; the spans are under the influence of each other by the slope of the control points that they have in common. The parametric interpolation method

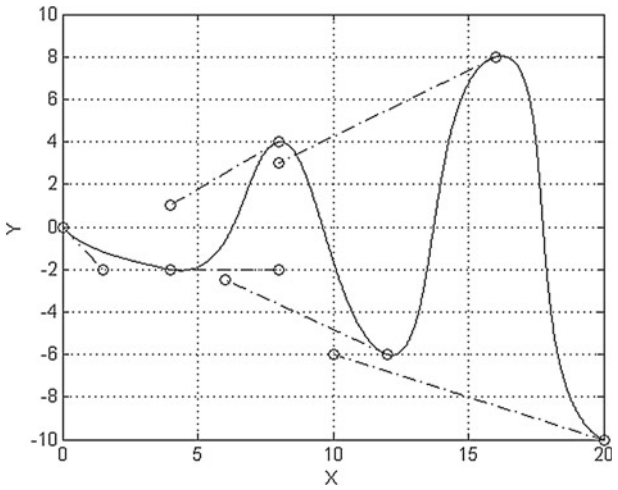

Fig. 2 An example of H-spline with 6 control points

of this spline is written below, and the equations are valid for one segment (i.e., a segment with two control points p_i and p_{i+1} as boundaries), and for each segment, these equations should be repeated. Thus if two points with their slopes are given for the ith span, then the blending function is written as:

$$p(u) = au^3 + bu^2 + cu + d, \tag{3}$$

$$a = 2P_i - 2P_{i+1} + P'_i + P'_{i+1}, \tag{4}$$

$$b = -3P_i + 3P_{i+1} - 2P'_i - P'_{i+1}, \tag{5}$$

$$c = P'_i, \tag{6}$$

$$d = P_i, \tag{7}$$

where u is the parametric variable and is between 0 and 1 in the segment, P_i and P_{i+1} are the coordinate positions of the control points i and $i+1$, respectively, P'_i and P'_{i+1} are the vector slopes of the control points that bound the ith segment.

Figure 2 shows an example of an Hermite spline with 6 control points having the coordinates $P_x = \{0.0 \quad 4.0 \quad 8.0 \quad 12.0 \quad 16.0 \quad 20.0\}^{\mathrm{T}}$ and $P_y = \{0.0 \quad -2.0 \quad 4.0 \quad -6.0 \quad 8.0 \quad -10.0\}^{\mathrm{T}}$ and with slopes $P'_x = \{1.5 \quad 8.0 \quad 4.0 \quad 6.0 \quad 8.0 \quad 10\}^{\mathrm{T}}$ and $P'_y = \{-2.0 \quad -2.0 \quad 1.0 \quad -2.5 \quad 3.0 \quad -6.0\}^{\mathrm{T}}$.

3 Elastic spline theory

In order to address the comparison between the two interpolation methods, some recalls about the theory of elastic splines are herein discussed. The formulation will be limited to the planar description of the curves.

For a mechanical system subjected to forces F_{ext} and constraints ψ, the static equilibrium can be studied using the Lagrangian approach, by minimizing the augmented Lagrangian function obtaining the following system of equations to be fulfilled:

$$\begin{cases} \nabla U + \psi_q^T \lambda - F_{\mathrm{ext}} = \{0\}, \\ \psi = \{0\}, \end{cases} \tag{8}$$

where

U is the elastic energy of the deformable bodies
ψ_q is the Jacobian matrix of the vector of the constraint equations ψ;
λ is the vector of Lagrange multipliers associated with the constraints ψ_i;
F_{ext} is the vector of the external applied loads.

The elastic equilibrium is found by solving for the values of the degrees of freedom q_i of the spline, which minimize the global elastic energy subjected to the vector ψ of constraints and applied loads F_{ext}.

In our two-dimensional case, the elastic energy U of a spline has two contributions [8,18]: stretching and bending:

$$U = U_{\text{stretching}} + U_{\text{bending}}. \tag{9}$$

Since the considered beam is very slender, the shear elastic energy can be neglected.
Each term in Eq. (9) can be written using material integrals:

– for the stretching elastic energy $U_{\text{stretching}}$ we have

$$U_{\text{stretching}} = \frac{1}{2} \int_{\text{spline}} EA \left(\varepsilon_{\text{s}} - \varepsilon_{\text{s}}^0\right)^2 \mathrm{d}s = \frac{1}{2} \int_0^1 EA \left(\varepsilon_{\text{s}} - \varepsilon_{\text{s}}^0\right)^2 \left\| \frac{\mathrm{d}p}{\mathrm{d}u} \right\| \mathrm{d}u, \tag{10}$$

where

E is the Young's modulus of the material;
A is the area of the cross section of the spline (it can vary throughout the length);
ε_{s}^0 is the stretching strain of the free form spline ($p(u) = p_0(u)$);
ε_{s} is the stretching strain of the deformed spline.

The exact (nonlinear) stretching strain can be evaluated as:

$$\varepsilon_{\text{s}}(u) - \varepsilon_{\text{s}}^0(u) = \ln \left(\frac{\left\| \frac{\mathrm{d}p}{\mathrm{d}u} \right\|}{\left\| \frac{\mathrm{d}p_0}{\mathrm{d}u} \right\|} \right). \tag{11}$$

– for the bending elastic energy U_{bending} we have

$$U_{\text{bending}} = \frac{1}{2} \int_{\text{spline}} EI \left(\varepsilon_{\text{b}} - \varepsilon_{\text{b}}^0\right)^2 \mathrm{d}s = \frac{1}{2} \int_0^1 EI \left(\varepsilon_{\text{b}} - \varepsilon_{\text{b}}^0\right)^2 \left\| \frac{\mathrm{d}p}{\mathrm{d}u} \right\| du, \tag{12}$$

where

ε_{b}^0 is the bending strain of the free form spline ($p(u) = p_0(u)$);
ε_{b} is the bending strain of the deformed spline;
I is the moment of inertia of the cross section with respect to the bending axis (the section is considered symmetrical, but it can vary throughout the length).

The bending strain is expressed by the scalar Frenet curvature $\kappa(u)$:

$$\varepsilon_{\text{b}}(u) = \kappa(u) = \frac{\left\| p'(u) \times p''(u) \right\|}{\left\| p'(u) \right\|^3}. \tag{13}$$

The presence of connections at the ends of the beam-shaped elements can be taken into account by introducing n algebraic equations ψ_i, describing the kinematic constraints (pin, fixture, slider, etc.).

The generalized forces F_{ext} associated with a generic external load can be computed using the virtual works.

Consider an applied force $\{F\}$ acting on a point M of the beam. Assuming u_M as the value of the parameter u in correspondence of M, the virtual work L of the force $\{F\}$ can be written as:

$$L = \{F\} \cdot \{\mathrm{d}M\} = \{F\} \cdot \{\mathrm{d}p(u_M)\}, \tag{14}$$

where $\mathrm{d}p(u_M)$ is the virtual displacement of point M expressed in terms of spline variations $\mathrm{d}q_i$.

The generalized external force component can be evaluated as:

$$Q_{i,F} = \frac{\partial L}{\partial q_i}. \tag{15}$$

Fig. 3 Cantilever beam

Table 1 Specifications of the considered Cantilever beam

Length	2.5 m
Circular cross-section radius	0.05 m
Elastic modulus	205.0 GPa
Poisson's ratio	0.29

4 Preliminary comparison: cantilever beam undergoing medium and large deflection

The first numerical simulation concerns a cantilever beam (shown in Fig. 3) with a vertical force applied to one of its ends. The scenario has been modeled with a B-spline using 6 control points (12 degrees of freedom) and with an H-spline with 3 control points (12 degrees of freedom, as well). The aim is to obtain the amount of deflection that is caused by the external load.

In both interpolation methods, 2 different values of the force have been applied in order to produce a medium and large nonlinear deflection. The geometrical and elastic properties of the beam are reported in Table 1.

The applied force is 25 kN for the medium deflection case and 250 kN for the large deflection case. The results of both simulations are also compared with a nonlinear finite element model.

4.1 Modeling a cantilever beam with a B-spline

A cubic B-spline with 6 control points (12 degrees of freedom) is used in order to describe the cantilever beam with the mentioned specifications. After applying the elastic spline equations throughout the spline, boundary conditions are added to the spline in order to fulfill the cantilever configuration.

The Frenet frame (tangent, normal and binormal vectors) [2] is considered to define the tangent vector at the first point of the beam and to impose the condition in which it is always orthogonal to the vertical unit vector, in order to prevent the beam from rotating. To have one side of the beam constrained, a relationship is imposed to keep the coordinates of the first point of the beam fixed. Thus, 2 constraint scalar equations (ψ_1 and ψ_2) are needed to prevent the translations of the first point and 1 scalar equation, ψ_3, to prevent the beam from rotating. Thus, the vector of constraining equations $\{\psi\}$ can be written as:

$$\psi_1 = X_1 = 0, \tag{16}$$

$$\psi_2 = Y_1 = 0, \tag{17}$$

$$\psi_3 = \left\{ t_x\,(u=0) \quad t_y\,(u=0) \right\} \cdot \left\{ 1 \quad 0 \right\}^{\mathrm{T}} = 0, \tag{18}$$

where the tangent vector t can be computed as

$$t\,(u) = \frac{p'\,(u=0)}{\|p'\,(u=0)\|}. \tag{19}$$

The location of the control points has been chosen not uniform in order to have more points in the region where a higher curvature is expected. The location of the initial undeformed position of the control points for this simulation is as follows:

$$P_x = \left\{ 0.00 \quad 0.25 \quad 0.50 \quad 1.25 \quad 2.00 \quad 2.50 \right\}^{\mathrm{T}},$$

$$P_y = \left\{ 0.00 \quad 0.00 \quad 0.00 \quad 0.00 \quad 0.00 \quad 0.00 \right\}^{\mathrm{T}}.$$

4.2 Modeling a cantilever beam with an Hermite spline

An Hermite spline with 3 control points (12 degrees of freedom) is implemented to apply the equations of the elastic spline, and the boundary conditions are applied in order to represent the behavior of a cantilever beam. The specifications of the beam are the same as in the previous case. Two types of static loads with the same amplitude of the previous simulations are considered for obtaining the same medium and large deflections.

In order to avoid pre-stressing of the beam, the amplitudes of the slopes of the control points have been initially set equal to the length of the segment that is between the two control points. This ensures that no initial stretching strain ε_s is present in the structure.

Moreover, the control points have been initially located at uniform distance. The initial control point positions and slopes are the following:

$$
\begin{aligned}
P_x &= \left\{ 0.0 \quad \frac{2.5}{2} \quad 2.5 \right\}^{\mathrm{T}}, \\
P_y &= \left\{ 0 \quad 0 \quad 0 \right\}, \\
P'_x &= \left\{ \frac{2.5}{2} \quad \frac{2.5}{2} \quad \frac{2.5}{2} \right\}^{\mathrm{T}}, \\
P'_y &= \left\{ 0 \quad 0 \quad 0 \right\}.
\end{aligned}
$$

The boundary conditions that are applied to the Hermite spline are expressed with the following constraint equations:

$$\psi_1 = X_1 = 0, \tag{20}$$

$$\psi_2 = Y_1 = 0, \tag{21}$$

$$\psi_3 = p'_x\,(u = 0) = P'_{1,x} = P_{2,x} - P_{1,x}, \tag{22}$$

$$\psi_4 = p'_y\,(u = 0) = P_{1,y} = 0. \tag{23}$$

4.3 Modeling a cantilever beam with finite elements

In order to compare the results coming from the two modeling strategies, the cantilever beam has also been modeled using finite elements. The beam has been discretized with 50 beam elements, and ABAQUS has been used to solve the system, taking into account geometrical nonlinearities and performing an incremental static analysis with the same number of steps.

4.4 Results comparison

The three modeling strategies (B-spline and H-spline formulations and finite elements) have been compared considering the results of the displacement and the magnitude of reaction forces. The finite element model has been assumed as a reference.

Figures 4 and 5 show comparative summaries of the results for the medium and large deflection cases, respectively.

The numerical comparison has been made by considering the percentage errors on the deflection of the free end of the beam (point of maximum displacement) computed with Eq. (22):

$$\text{Error} = \frac{(\delta_{\text{FEM}} - \delta_{\text{spline}}) \times 100}{\delta_{\text{FEM}}}\,\%. \tag{24}$$

The same comparison is also carried out for the reaction moments, in which the moment obtained by the interpolation methods is compared to that obtained by the finite element model.

Tables 2 and 3 report the complete set of comparisons, considering also intermediate points, for the medium and large deflection cases, respectively.

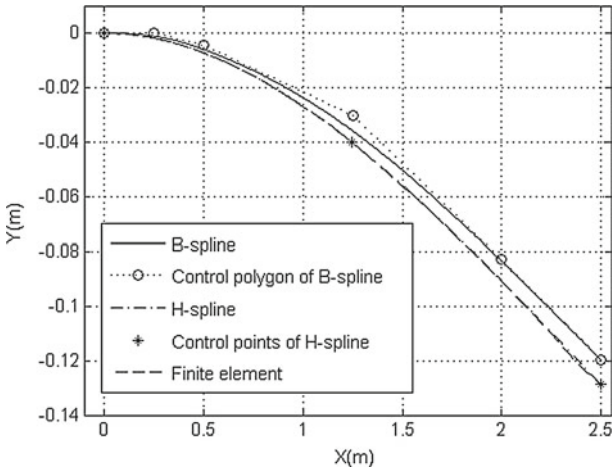

Fig. 4 Comparison of the deflection of the cantilever beam under 25 kN load using finite element, H-spline and B-spline formulations

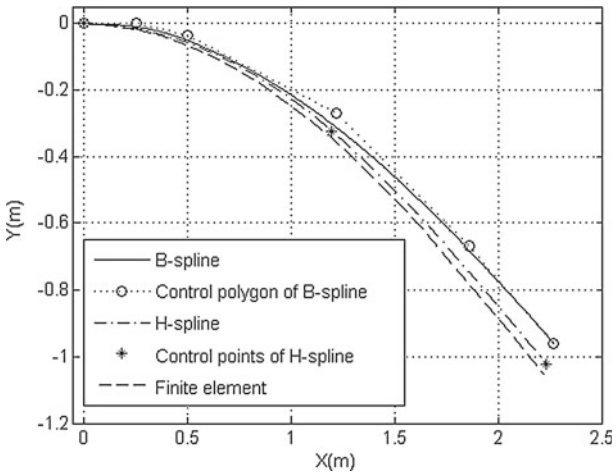

Fig. 5 Comparison of the deflection of the cantilever beam under 250 kN load using finite element, H-spline and B-spline formulation

Table 2 Resultant displacements, reaction forces and maximum error of B-spline, H-spline and finite elements for the cantilever beam under 25 kN load

Location of beam	B-spline	H-spline	Finite elements
$0L$	0.0 m	0 m	0 m
$(1/4)L$	0.010 m	0.011 m	0.011 m
$L/2$	0.036 m	0.040 m	0.040 m
$(3/4)L$	0.075 m	0.0812 m	0.0818 m
$L = 2.5$ m	0.12 m	0.1284 m	0.1290 m
Reaction forces	$Rx = 0$ N	$Rx = 0$ N	$Rx = 0$
	$Ry = 25$ kN	$Ry = 25$ kN	$Ry = 25$ kN
	$Mz = 62{,}410.2$ Nm	$Mz = 62{,}355.5$ Nm	$Mz = 62{,}399.4$ Nm
Error on reaction moment (%)	0.02	0.07	–
Error on maximum displacement (%)	7.0	0.5	–

For a medium deflection, it was noticed that the B-spline formulation gives an error in the estimation of the beam free end deflection of 7 % and the H-spline a very good accordance with only 0.5 % difference.

For the large deflection, it was noticed that the B-spline formulation gives an error in the estimation of the beam free end deflection of 9 % and the H-spline a better accordance with 3.0 % difference. To obtain the results of large deflection, the required load (250 kN) was iteratively applied by giving an increase of 50 kN in each step, while for the medium deflection, iterative loading (25 kN) was not required (single solving iteration).

Table 3 Resultant displacements, reaction forces and maximum error of B-spline, H-spline and finite elements for the cantilever beam under 250 kN load

Location of beam	B-spline	H-spline	Finite elements
$0L$	0.0 m	0.0 m	0.0 m
$(1/4)L$	0.081 m	0.086 m	0.080 m
$L/2$	0.303 m	0.320 m	0.343 m
$(3/4)L$	0.609 m	0.650 m	0.678 m
$L = 2.5$ m	0.959 m	1.020 m	1.053 m
Reaction forces	$Rx = 0.0$ N	$Rx = 0.0$ N	$Rx = 0.0$ N
	$Ry = 250$ kN	$Ry = 250$ kN	$Ry = 250$ kN
	$Mz = 565{,}918.3$ Nm	$Mz = 531{,}107.5$ Nm	$Mz = 553{,}982.0$ Nm
Error on reaction moment (%)	2.15	4.13	–
Error on maximum displacement (%)	9.0	3.0	–

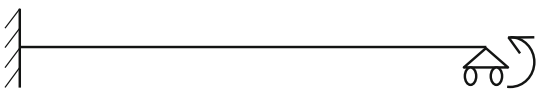

Fig. 6 A beam fixed at the *left side* and constrained to move horizontally on its *right side*, with an enforced rotation of 360° applied at its *right side*

Table 4 Specifications of the considered beam

Length	2.5 m
Circular cross-section diameter	0.5 mm
Elastic modulus	10.0 MPa
Poisson's ratio	0.29

5 Complex nonlinear study case

In order to compare the two interpolation methods in a more complex nonlinear case, a different test case has been implemented. It is about a beam fixed at one side and with the other end constrained to move horizontally (on an ideal slider), as depicted in Fig. 6. An enforced rotation of 360° is then incrementally applied to the sliding end.

The properties of the beam are reported in Table 4.

5.1 Modeling the beam with B-spline

The dynamic spline equations are applied to the cubic B-spline interpolation method with 20 control points $P_0 \ldots P_{19}$ (40 degrees of freedom). The boundary conditions that describe the fixed constraint are similar to the previous cantilever beam case. In order to prevent the vertical movement of the right side of the beam, another constraint is defined. Thus, Eqs. (16), (17) and (18) are still included and the following condition has been added:

$$\psi_4 = p_y\,(u = 1) = P_{19,y} = 0. \tag{25}$$

In order to apply the 360° rotation to the right end of the beam, a driving constraint is introduced by imposing the perpendicularity between a reference vector d and the tangent vector of the end point (i.e., at length L). Thus, by applying a full rotation of the vector d by increments, the tangent vector of the end point will rotate as well. With this procedure, a full rotation is applied, and the corresponding driving constraint equation is as follows:

$$\psi_5 = (t_x\,(u = 1) \cdot d_x) + \left(t_y\,(u = 1) \cdot d_y\right) = 0, \tag{26}$$

where d is the reference vector and is defined as

$$d = \begin{Bmatrix} \cos\alpha \\ \sin\alpha \end{Bmatrix}, \tag{27}$$

where α is the angle of rotation that increments from 90° to 450° in order to make a full rotation.

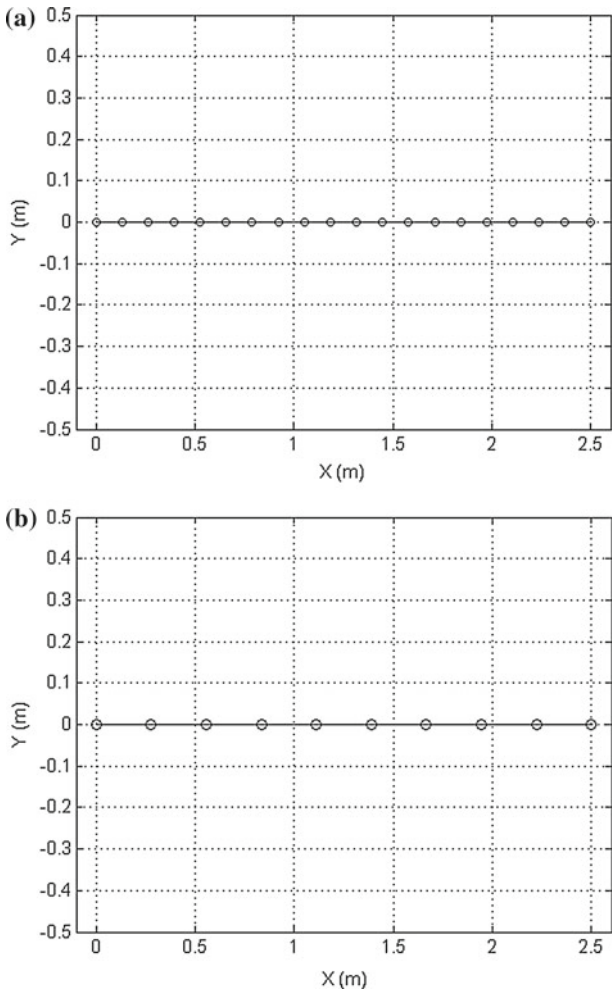

Fig. 7 The initial shape (before applying the enforced rotation) of the beam modeled with B-spline with 20 control points (**a**) and H-spline with 10 control points (**b**)

The control points have been initially distributed equally throughout the spline as shown in the initial configuration of Fig. 7a.

5.2 Modeling the beam with H-spline

A Hermite spline with 10 control points $P_0 \ldots P_9$ (40 degrees of freedom) is used in order to simulate the complex nonlinear study. For the initial configuration, the control points have been equally distributed as shown in Fig. 7b. For the definition of the initial slopes, each point possesses an initial slope aligned to the X axis with an amplitude equal to the length of the segment (1/9 of the length of the beam). To maintain a fixed position of the right end, the same constraint equations that have been used in the cantilever beam case are applied, by using Eqs. (20), (21), (22) and (23). In order to describe the sliding end, the following equation has been added:

$$\psi_5 = p_y\,(u = 1) = P_{9,y} = 0. \tag{28}$$

The enforced rotation has been imposed with a constraint equation with the same strategy of the procedure defined in the previous Sect. 5.1, expressed by:

$$\psi_6 = \left(P'_{9x} \cdot d_x\right) + \left(P'_{9y} \cdot d_y\right) = 0, \tag{29}$$

where d is again the rotating reference vector.

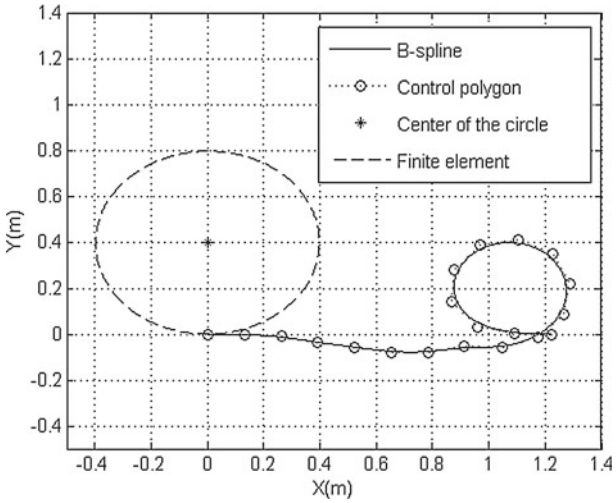

Fig. 8 The final shape of the beam coming from the B-spline formulation with 20 control points compared to that of the finite elements

5.3 Implementing finite element to the nonlinear case study

In order to compare the results coming from the two modeling strategies, the beam was modeled using finite elements. Since the expected displacement is very high, 500 beam elements have been used. The driving constraint has been applied with an enforced rotation. ABAQUS has been used for solving, performing an incremental static analysis with the same number of steps of the spline simulations.

5.4 Comparing the obtained results after applying a full rotation

The results of the finite element simulation show that the final shape of the beam after the full rotation is quite a perfect circle. For the B-spline formulation, the results of the simulation are depicted in Fig. 8, together with those coming from finite elements. It can be noticed that the final shape is very much different from the one that is obtained using finite elements, and a full circle is not achieved at all. In fact, the first half of the beam is almost straight, and a curl is formed only near the right end. It should be mentioned that the enforced rotation was applied with iterations with an increase of 0.5° at each step.

Figure 9 shows the comparison between the H-spline formulation and finite elements. In this case, the results are very similar and a full circle is obtained with a very good accuracy.

It was noticed that the amount of error that was estimated throughout the final shape was $<1\,\%$, in comparison with the results of the finite element model.

6 Discussion

By the interpretation of the two test cases, an overall comparison between the B-spline and the H-spline can be addressed in order to underline the pros and cons of each method.

First of all, all the simulations have been performed considering the same number of degrees of freedom in order to have a more consistent comparison.

Although the B-splines can be described with an easier mathematical structure, they are suitable only for limited range of displacement. Passing from a medium to a large nonlinear deformation field, the B-spline would require a greater number of control points.

On the other hand, for a slightly nonlinear simulation, they are able to describe the elasticity of the structure in a satisfactory manner.

Actually, several simulations have been repeated by varying the initial spacing between control points, and differences have been noticed. A concentration of points in the zones of higher curvature has a benefit on the accuracy of the results. Table 5 collects the results of some of these numerical experiments, which have been

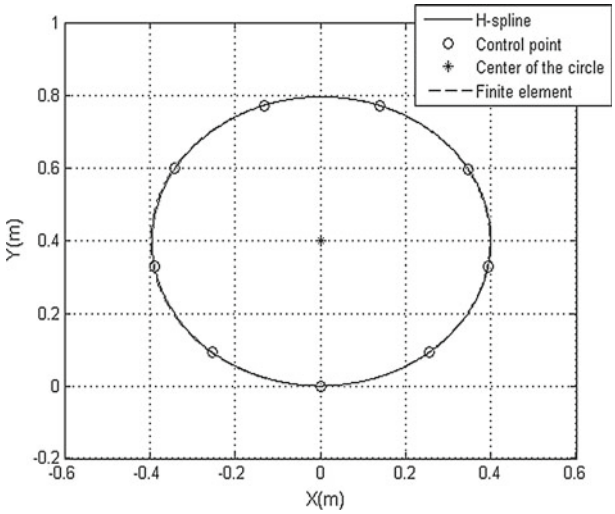

Fig. 9 The final shape of the beam coming from the H-spline formulation with 10 control points compared to that of finite elements

Table 5 The effect of spacing of the initial position of the control points on the cantilever beam modeled using a B-spline with 6 control points loaded with 250 kN

Initial location of the control points	Free end deflection (m)	Error (reference FEM value 1.053 m) (%)
(Equal distance distribution)	0.865	17.9
$p_x = \{0 \ \frac{L}{5} \ \frac{2L}{5} \ \frac{3L}{5} \ \frac{4L}{5} \ L = 2.5\}^{\mathrm{T}}$		
$p_y = \{0 \ 0 \ 0 \ 0 \ 0 \ 0\}^{\mathrm{T}}$		
$p_x = \{0 \ 0.025 \ 0.5 \ 1.25 \ 2 \ 2.5\}^{\mathrm{T}}$	0.959	9
$p_y = \{0 \ 0 \ 0 \ 0 \ 0 \ 0\}^{\mathrm{T}}$		
$p_x = \{0 \ 0.5 \ 0.9 \ 1.25 \ 2 \ 2.5\}^{\mathrm{T}}$	0.806	23.5
$p_y = \{0 \ 0 \ 0 \ 0 \ 0 \ 0\}^{\mathrm{T}}$		
$p_x = \{0 \ 0.25 \ 0.5 \ 0.9 \ 1.25 \ 2.5\}^{\mathrm{T}}$	0.929	11.8
$p_y = \{0 \ 0 \ 0 \ 0 \ 0 \ 0\}^{\mathrm{T}}$		

compared to those of the finite element model. On the other hand, an optimization would require an iterative process or a self-adjusting procedure, including excessive complications and partially losing the generality of the methods.

The benefits of the B-spline are mainly two. The first one is related to the geometrical description. Expressing a curve using a B-spline (or the similar rational expression [2]) is very common and so the direct relationship geometrical entity–analysis entity is more direct. The other advantage is that the B-spline requires the definition of just point coordinates (x and y) and there is no need for any other less-intuitive information such as the values of the slope at each control point. For the same reason, the mathematical implementation is easier and more compact with respect to the H-spline, requiring less time to be solved. Moreover, the reaction moment and forces obtained from the B-spline formulation show a slightly better accuracy with respect to the H-spline one.

The H-spline formulation has revealed to be more robust and accurate compared to the B-spline even for very large displacements. Unlike the B-spline formulation, the distribution of the control points at the initial position in the Hermite splines do not require specific attention and a uniform distribution has revealed to be suitable for all kinds of problem. The only requirement is that the initial values of the slopes have to be equal to the length of the corresponding segment.

The main drawback of the H-spline formulation is that it is time-consuming, and thus, the execution of the simulation requires more time in order to achieve the final result. All the numerical codes have been developed in MATLAB language, and in general, the time required for the computer to solve the H-spline problem is twice the time that is needed to process the B-spline formulation.

7 Conclusion

In this paper, two different interpolation strategies have been compared for the application with the elastic spline numerical simulations. Both the investigated formulations are suitable for the assessment of the mechanical behavior of slender elements allowing the definition of even a very large displacement using a limited set of parameters with respect to the standard finite element approach. By choosing the spline descriptors, it is possible to use the same mathematical entities for both geometrical modeling and structural simulations. The compared formulations are based on Bézier and Hermite interpolation, and they both have been implemented and tested on two simulation cases. The results of the study show that the B-spline allows a more compact and less complex implementation but requires a precise choice of the location of the control points and a less accurate solution especially for very high nonlinear simulations. Based on these considerations, the choice of one of the two formulations can be done according to the complexity and the amplitude of the deformation.

The method of elastic splines, and its extension including inertial effects (the so-called dynamic spline), can be used for flexible multibody simulations and in the design and analysis of complaint mechanisms.

References

1. Qin, H., Terzopoulos, D.: D-NURBS: a physics-based framework for geometric design. IEEE Trans. Vis. Comput. Graph. **2**(1), 85–96 (1996)
2. Farin, G.: Curves and Surfaces for CAGD, 5th edn. Morgan Kaufmann Publishers, San Francisco, CA (2002)
3. Hughes, T.J.R., Cottrell, J.A., Bazilevs, Y.: Isogeometric analysis: CAD, finite elements, NURBS, exact geometry, and mesh refinement. Comput. Methods Appl. Mech. Eng. **194**, 4135–4195 (2005)
4. Cottrell, J.A., Reali, A., Bazilevs, Y., Hughes, T.J.R.: Isogeometric analysis of structural vibrations. Comput. Methods Appl. Mech. Eng. **195**, 5257–5297 (2006)
5. Theetten, A., Grisoni, L., Andriot, C., Barsky, B.: Geometrically exact dynamic splines. Comput.-Aided Des. **40**, 35–48 (2008)
6. Nagy, A.P., Abdalla, M.M., Gürdal, Z.: Isogeometric sizing and shape optimisation of beam structures. Comput. Methods Appl. Mech. Eng. **199**, 1216–1230 (2010)
7. Benson, D.J., Bazilevs, Y., De Luycker, E., Hsu, M.-C., Scott, M., Hughes, T.J.R., Belytschko, T.: A generalized finite element formulation for arbitrary basis functions: From isogeometric analysis to XFEM. Int. J. Numer. Methods Eng. **83**, 765–785 (2010)
8. Valentini, P. P., Pennestrì, E.: Modelling elastic beams using dynamic splines. Multibody Syst. Dyn. **25**(3), 271–284 (2011)
9. Valentini, P.P., Pezzuti, E.: Design and interactive simulation of cross-axis compliant pivot using dynamic splines. Int. J. Interact. Des. Manuf. doi:10.1007/s12008-012-0180-x
10. Valentini, P.P.: Modelling human spine using dynamic spline approach for vibrational simulation. J. Sound Vib. **331**, 5895–5909 (2012)
11. Bouclier, R., Elguedj, T., Combescure, A.: Locking free isogeometric formulations of curved thick beams. Comput. Methods Appl. Mech. Eng. **1**, 245–246
12. Raknes, S.B., Deng, X., Bazilevs, Y., Benson, D.J., Mathisen, K.M., Kvamsdal, T.: Isogeometric rotation-free bending-stabilized cables: statics, dynamics, bending strips and coupling with shells. Comput. Methods Appl. Mech. Eng. In press. doi:10.1016/j.cma.2013.05.005
13. Weeger, O., Wever, U., Simeon, B.: Isogeometric analysis of nonlinear Euler–Bernoulli beam vibrations. Nonlinear Dyn. **72**, 813–835 (2013)
14. Shabana, A.A.: Definition of the slopes and the finite element absolute nodal coordinate formulation. Multibody Syst. Dyn. **1**(3), 339–348 (1997)
15. Von Dombrowski, S.: Analysis of large flexible body deformation in multibody systems using absolute coordinates. Multibody Syst. Dyn. **8**, 409–432 (2002)
16. Berzeri, M., Shabana, A.: Development of simple models for the elastic forces in the absolute nodal co-ordinate formulation. J. Sound Vib. **235**(4), 539–565 (2000)
17. Sanborn, G.G., Shabana, A.A.: On the integration of computer aided design and analysis using the finite element absolute nodal coordinate formulation. Multibody Syst. Dyn. **22**, 181–197 (2009)
18. Valentini, P.P., Hashemi-Dehkordi, S.M.: Effects of dimensional errors on compliant mechanisms performance by using dynamic splines. Mech. Mach. Theory **70**, 106–115 (2013)